Dalton Transactions

Cite this: *Dalton Trans.*, 2012, **41**, 2632

www.rsc.org/dalton

PAPER

Structural, odd–even chain alternation and thermal investigation of a homologous series of anhydrous silver(I) n-alkanoates

Peter Nattaniel Nelson and Henry Anthony Ellis*

Received 30th August 2011, Accepted 24th November 2011
DOI: 10.1039/c2dt11638c

Molecular and lattice structures of a homologous series (n_c = 8–20, inclusive) of silver (I) n-alkanoates are determined from X-ray Powder Diffraction, Solid State spin decoupled ^{13}C-NMR and variable temperature Fourier Transform Infrared Spectroscopies. The compounds crystallize in a monoclinic crystal system with hydrocarbon chains in the fully extended all-*trans* conformation. Moreover, the chains are tilted *ca.* 75° with respect to the metal basal plane and are arranged as methyl(tail)-to-methyl(tail) bilayers within a lamellar. The methyl chain ends, from different layers in the bilayer, do not overlap but are in such close proximity to cause methyl–methyl interactions. In a molecule, two carboxylate groups bind in a *syn–syn* type bridging bidentate mode to two silver atoms to form an eight-membered structure. Intramolecular silver–silver and intermolecular Ag–O–Ag interactions stabilize the head group and promote the formation of layer type polymeric sheets. Though the compounds are nearly isostructural, odd–even chain alternation is observed in density, anti-symmetric stretching vibrations of methyl and unusually, carboxylate (head) groups, as a result of packing differences of hydrocarbon chains within the crystal lattice. These arise from the relative vertical distances between polymeric sheets, which are not in the same plane. Thus, for odd chain length compounds, where those distances are less than for even chains, more ordered packing and hence higher densities are observed for these adducts. Also, the numbers and natures of the thermotropic phase transitions are chain length dependent and irreversible.

Introduction

The structural chemistry of metal carboxylates (soaps) is very interesting because of the various coordination possibilities presented by the central metal ion. These compounds are used extensively, as catalysts, dryers, polymer stabilizers and as coating agents for preventing corrosion in metals.[1,2] In the case of silver soaps, these find ready application, especially the octadecanoate and docosanoate, as photothermographic (PTG) imaging materials. As they are a source of metallic silver nanoparticles, they are suitable for use as the imaging agent.[3] Though their room temperature molecular structures have been investigated, extensively,[4–6] only the short chain length silver acetate and propanioate were determined definitely, by single crystal XRD.[6,7] Both compounds were reported to exist as dimeric monomers (Ag_2(carboxylate)$_2$) in which each carboxylate group was coordinated to silver atoms by bridging bidentate bonding. Each molecular unit was connected by inter-dimer silver–oxygen–silver interactions between adjacent molecules to form chains that are aligned parallel to each other. Moreover, the silver–silver distance, at *ca.* 2.9 Å,[6] is well within the silver–silver distance in metallic silver. This suggests that silver–silver bonds are formed within the dimeric complex. Various views on the possibility of forming such bonds have been the subject of much discussion.[8–10] However, the preponderance of evidence supports silver–silver bonds. For these, there are four molecules per unit cell arranged in a triclinic[4,6] or monoclinic[7] crystal system.

Despite the importance of long chain length soaps in PTG applications, not much is known about their molecular structures and lattice packing characteristics. Because these soaps are of low symmetry, they do not readily form single crystals for X-ray diffraction (XRD) studies. Rather, the long chain length compounds form white microcrystalline powders that are light sensitive. Nevertheless, molecular structures were proposed, from powder XRD, for silver(I) propanoate to octacosanaoate, inclusive.[5] For these, hydrocarbon chains are arranged in a tail-to-tail bilayer, within a lamellar, with chains perpendicular to the metal basal plane. However, not much has been reported on the packing of hydrocarbon chains in the crystal lattice and the influence of odd–even chains on such packing. Hence, a detailed study of lattice packing, chain length effects and their influence on thermal behaviour is warranted.

In this paper, variable temperature FT-infrared and solid- state ^{13}C NMR spectroscopies, in conjunction with powder XRD, have been used to investigate chain length effects on hydrocarbon chain packing, within the crystal lattice, in silver(I) n-alkanoates, from octanoate to eicosanoate, inclusive, to produce a more complete molecular model than hithertofore.[5] Additionally, the influence of chain length, whether odd or even, on the thermal properties of these soaps is discussed.

Department of Chemistry, University of the West Indies, MonaKingston 7, Jamaica. E-mail: henry.ellis@uwimona.edu.jm

Table 1 Elemental analyses for anhydrous silver n-alkanoates

	Carbon/%		Hydrogen/%	
Compound	Experimental	Calculated	Experimental	Calculated
AgC_8	38.18	38.27	5.82	6.08
AgC_9	40.77	40.78	6.19	6.46
AgC_{10}	42.15	43.03	6.94	6.86
AgC_{11}	45.13	45.07	7.50	7.22
AgC_{12}	46.92	46.92	7.71	7.55
AgC_{13}	48.58	48.61	8.17	7.84
AgC_{14}	50.07	50.17	8.51	8.12
AgC_{15}	51.59	51.58	8.76	8.37
AgC_{16}	53.47	52.90	8.71	8.60
AgC_{17}	54.63	54.12	9.38	8.82
AgC_{18}	55.68	55.24	9.17	9.01
AgC_{19}	56.60	56.30	9.76	9.20
AgC_{20}	57.67	57.28	9.81	9.37

Results and discussion

The purity of the soaps was confirmed by elemental analysis (Table 1) and IR spectroscopy. The experimentally determined carbon and hydrogen values are in excellent agreement with calculated values. Representative IR spectra, collected at room temperature, are shown in Fig. 1. The absence of a carbonyl adsorption band in the region of *ca.* 1700 cm^{-1} and its replacement by carboxylate absorptions between 1520–1410 cm^{-1} indicates that the compounds are free of acid. Also, there is complete resonance in the C–O bonds of the carboxylate groups, resulting from its coordination with silver. Moreover, the absence of hydroxyl absorptions between 3500–3300 cm^{-1} confirms that the compounds are anhydrous. The spectra are fairly similar and typical for metal carboxylates.[14] Of interest are strong bands in the region of 1700–1200 cm^{-1} and medium to weak bands between1400–500 cm^{-1}. These weak bands are ascribed to methylene progressive absorptions. Also, symmetric (ν_s) and asymmetric (ν_{as}) methyl (CH_3) and methylene (CH_2) bands are found in the region of 2960–2840 cm^{-1}. Additionally, the progression of regularly spaced narrow bands, between 1345–1100 cm^{-1}, are the wagging vibrations of CH_2 groups and

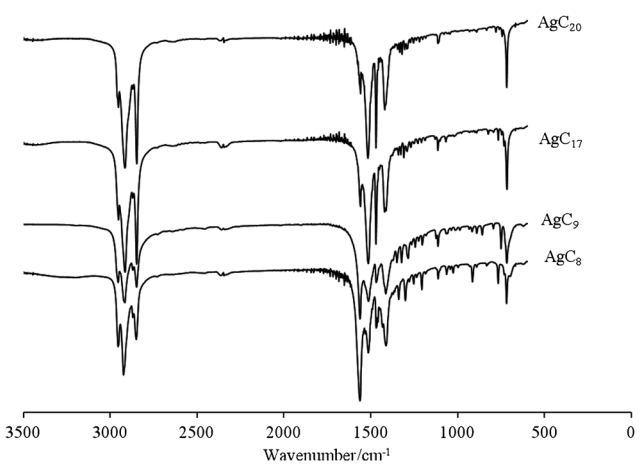

Fig. 1 Representative room temperature IR spectra for anhydrous silver n-alkanoates.

indicate that the hydrocarbon chains are in the all-*trans* conformation.[15–17] Indeed, further detailed analyses of the spectra provide information on lattice packing of hydrocarbon chains, head group bonding and intermolecular interactions in the crystal lattice.[16,18,19] Important indicators are: symmetric, ν_s COO *ca.* 1520 cm^{-1} and asymmetric, ν_{as} COO *ca.* 1410 cm^{-1}, carbonyl stretches as well as methylene group in-plane rocking, ρCH_2 at *ca.* 717 cm^{-1} and methylene bending, τCH_2 at ~1470–1472 cm^{-1} vibrations. For example, the type of hydrocarbon packing can be ascertained from the shapes of the CH_2 absorption bands. In this case, since both bands are split, the clear inference is that hydrocarbon chains crystallize in a monoclinic or orthorhombic crystal system.[15,16,20] Also, the split in the methyl group asymmetric band is clearly due to methyl group intermolecular interactions rather than the presence of two distinct crystallographic chains. For all compounds, $\nu_{as}CH_3$ and ν_s CH_3 are found in the narrow range of 2956–2957 and 2880–2870 cm^{-1} respectively. The remaining two absorptions in the region of 2950–2925 and 2849–2848 cm^{-1} are assigned to $\nu_{as}CH_2$ and ν_s CH_2, respectively. However, for crystalline n-alkanes, in the fully extended all-*trans* conformation, ν_s CH_2 and ν_{as} CH_2 are found at 2916 and 2947 cm^{-1}.[15] This indicates that the hydrocarbon chains are *ca.* 99.8% in the all-*trans* conformation. Furthermore, the splitting of ν_{as} CH_3, in all compounds, indicates a decrease in symmetry of the methyl group as a result of intermolecular interactions between hydrocarbon chains.[15,18,21] However, the extent of these van der Waal interactions is influenced by odd or even chain lengths. For example, ν_{as} CH_3 absorptions occur at higher frequencies for even chain length adducts. This is clear evidence for methyl–methyl and or methyl–methylene interactions between chains from opposite layers in a bilayer. Thus, for all compounds, the hydrocarbon chains are arranged in a bilayer, within a lamellar. In all compounds, the ν_{as} COO band is more intense than ν_s COO, indicating an asymmetric arrangement of carboxylate groups around the metal ion and indicate tilting of hydrocarbon chains within the lamellar. Moreover, both bands are split; which is clear evidence for head group interactions between adjacent molecules. Indeed, Olson and coworkers,[6] in their study of the crystal structure of silver acetate, reported extensive head group interactions and intra-molecular silver–silver bonds. The results here, unlike those reported,[5] indicate head group and silver–silver interactions at all chain lengths, resulting in a lowering of head group symmetry. Furthermore, the frequency shift of these two bands, in conjunction with their relative positions, $\Delta\nu = \nu_{as} - \nu_s$ *ca.* 109 cm^{-1}, compared to free ions Na^+ and K^+ soaps is lower than expected and confirms intermolecular interactions. Interestingly, odd–even alternation is observed for both $\nu_{as}CH_3$ and $\nu_{as}COO$ absorptions (Fig. 2). Indeed, odd–even alternation in $\nu_{as}COO$ absorption has never been reported for any metal carboxylates. It is clear that even chain adducts occur at higher frequencies, possibly, in the case of $\nu_{as}CH_3$ as a result of the relative difference in closeness of approach of hydrocarbon chains from different layers in the bilayer.

Additional information on molecular interaction and chain packing can be adduced from high resolution ^{13}C NMR spectroscopy. Accordingly, typical spectra are shown in Fig. 3 for AgC_9, AgC_{14} and AgC_{17}. All spectra show six electronically distinct environments: carboxyl carbon (C1) at *ca.* 177 ppm, carbon

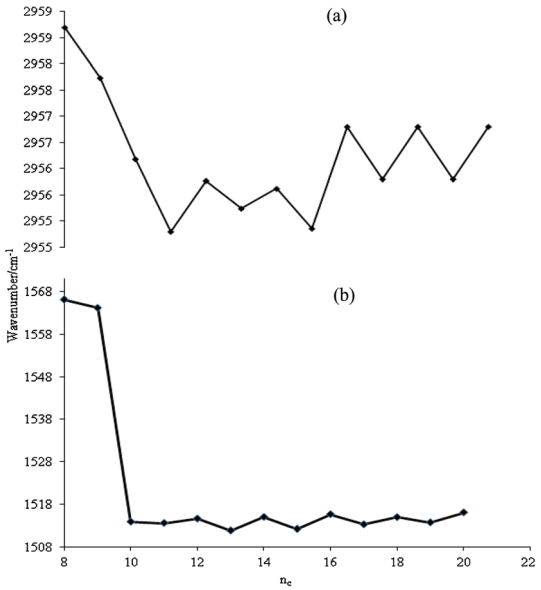

Fig. 2 Stretching frequencies for (a) ν_{as} CH_3 and (b) ν_{as} COO with chain length.

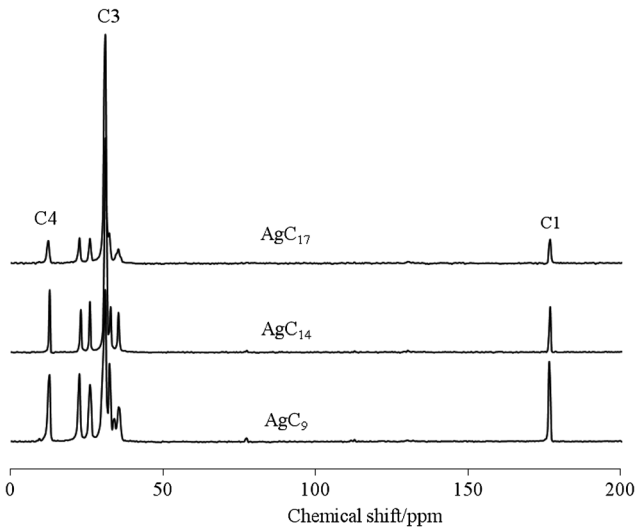

Fig. 3 Solid state ^{13}C-NMR spectra for selected compounds at room temperature.

adjacent to carboxyl carbon (C2) at *ca.* 35 ppm, cumulative methylene group carbons (C3) at *ca.* 31 ppm, terminal methyl carbons (tail); C4) at *ca.*12.5 ppm, and the other two carbons closest to methyl carbons at *ca.* 22.5 and 25.6 ppm. The very intense C3 resonance is ascribed to CH_2 groups in the hydrocarbon chains whose electronic environment is so similar that they are indistinguishable. However, as chain length decreases the electron density distribution in the polymethylene chains becomes more uneven. Hence, the cumulative CH_2 groups become better resolved at these chain lengths. Again, odd–even alternation is observed for methyl carbon resonances, as shown in Fig. 4(a). The chemical shifts for even chain length compounds are all higher than their odd adducts; that is, they are more deshielded. This could be a result of van der Waal interactions between closely packed methyl groups, from opposite

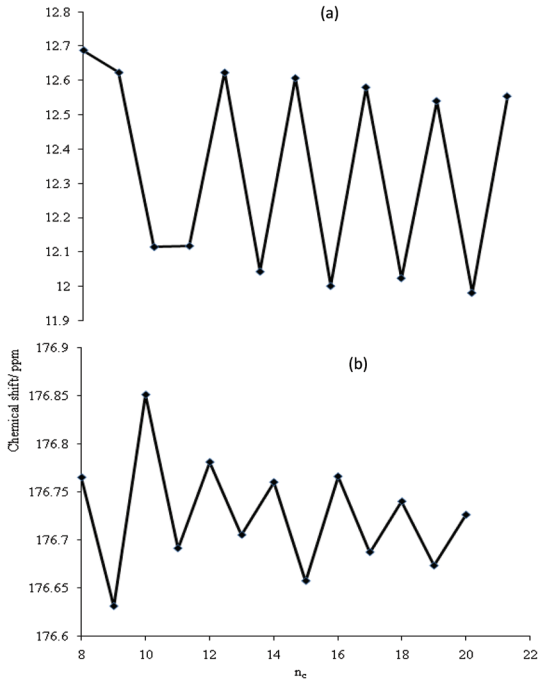

Fig. 4 Chemical shift for (a) CH_3 and (b) COO with chain length.

layers in the bilayer. That observation is supported by odd–even alternation observed in anti-symmetric stretching vibrations of methyl groups. Furthermore, odd–even alternation is observed for the chemical shifts of carbon in the carboxylate group (Fig. 4 (b); head group). Indeed, odd–even alternation in head group chemical shifts has never been reported. In the case of carboxyl groups, a higher electron density on carbonyl carbons of odd chain length compounds, arise from higher resonance in C–O bonds of carboxyl groups. Thus, higher metal–carboxylate interactions are inferred and ν_a COO absorptions are lowered. Furthermore, the higher resonance in C–O bonds, for odd chain lengths, results in higher electron density and hence the carboxyl carbon is more shielded.

X-ray powder diffraction peaks are shown in Fig. 5 as intensity *versus* diffraction angle, 2θ. These patterns were collected at room temperature. The low angle peaks are regularly spaced and intense with calculated d values in the ratio:$1 : 1/2 : 1/3 \ldots . : 1/n$, consistent with diffraction from a lamellar structure.[15,22–25] However, at angles in the range of $20° \leq 2\theta \leq 25°$, where side chain reflections are expected[26] very few low intensity or no reflections are observed. This is not in accord with the work of Binnemans and coworkers,[5] where extensive side chain interactions were observed for silver behenate. Moreover, unlike lithium[27] and zinc[18] n-alkanoates, the diffuse or no diffraction peaks, here reported, show no discernible patterns for odd and even chain lengths. However, evaluation of the diffraction patterns were carried out using Diffrac ^{plus} EVA 9.0 software (part of the machine operating system). Background subtraction (curvature: threshold of 1 : 1), K_α stripping (ratio 0.5) and profile smoothing (smooth factor = 0.15) were carried out. Diffraction peaks were chosen for indexation based on peak intensities and shapes. The data were then converted to a line profile diagram, by the software, for auto indexing. Further, the lines were indexed using commercially available Win-metric LS V2.1

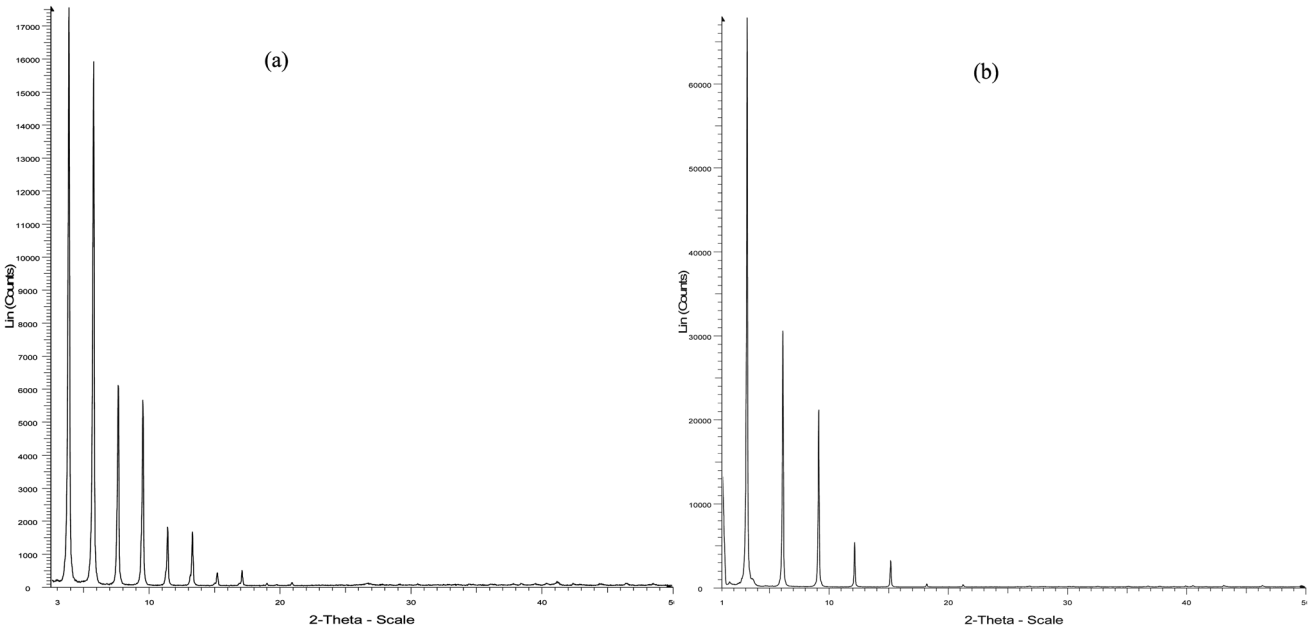

Fig. 5 Room temperature X-ray powder diffractograms for (a) silver heptadecanoate and (b) decanoate.

Table 2 Lattice parameters, experimental and calculated *d*-spacing data for anhydrous silver n-alkanoates

Compound	*a*/Å	*b*/Å	*c*/Å	*β* (°)	*V*/Å^3	d_{exp}/Å	$2d_L$/Å
AgC_8	5.05	4.32	24.26	93.27	528.80	24.21	24.56
AgC_9	5.30	4.46	27.25	94.27	641.80	27.18	27.08
AgC_{10}	5.94	4.03	29.38	94.16	702.03	29.30	29.61
AgC_{11}	5.85	4.05	32.00	93.40	756.74	31.95	32.13
AgC_{12}	5.97	4.23	34.19	91.50	860.13	34.18	34.65
AgC_{13}	6.01	4.01	37.00	91.08	891.68	36.99	37.18
AgC_{14}	6.22	6.23	38.99	91.19	1012.79	38.98	39.70
AgC_{15}	6.02	6.02	41.85	92.80	1036.09	41.80	42.22
AgC_{16}	6.82	6.82	43.82	91.69	1193.57	43.80	44.74
AgC_{17}	7.93	7.93	47.12	92.70	1484.89	47.06	47.27
AgC_{18}	8.10	4.94	48.98	90.21	1957.60	48.98	49.79
AgC_{19}	8.07	5.04	51.71	91.31	2102.88	51.67	52.31
AgC_{20}	10.74	5.62	54.18	94.22	3262.42	54.02	54.84

software for Windows at a tolerance of 0.1. The indexation process was completed by refining at lower tolerances. All the compounds crystallize in a monoclinic system with possibly P symmetry. The unit cell parameters, collected in Table 2, show that the principal axis is the *c* axis, which increases linearly with chain length ($r^2 = 0.999$). Importantly, the powder data and analyses are validated by the excellent agreement in lattice parameters when the data is used to predict the length of the *c* axis for silver propionate, obtained from single crystal data.[6,7] The distance between two consecutive metal basal planes, d_{exp} is determined from 001 reflections and molecular lengths, d_L from standard bond lengths and angles.[18] The room temperature data, given in Table 2, show $2d_L > d_{exp}$, indicative of chain tilting and or interdigitated within a lamellar. Interdigitation can be ruled out since there is no evidence of methyl–methylene interactions. However, there is a preponderance of evidence in favour of chain tilting at these temperatures.[23,25] This is not in accord with Binnemans *et al.*[5,27] structural models which proposed that hydrocarbon chains were perpendicular to the silver basal plane.

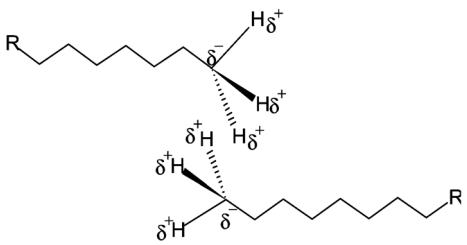

Scheme 1

One explanation is to propose the presence of undetected water in the crystal lattice which caused it to expand and make $d_{exp} > 2d_L$. However, this explanation is unlikely to be correct since, at the basal plane, the CO bonds of carboxylate groups are asymmetrically coordinated to silver. For perpendicular chains, the intensities of carboxyl absorptions would be equivalent. Clearly, a tilt angle, *r* for hydrocarbon chains of *ca.* 75°, relative to the metal basal plane, is in line with the results for other soaps.[5,12,16,23]

The distance between hydrocarbon chains ends, from different layers in the lamellar, D_{bt} is given by:

$$D_{bt} = (d_{exp}/\sin r) - 2d_L,$$

which gives a value for D_{bt} of *ca.* 0.9 Å, irrespective of chain length. Since the length of the C–H bond in a tail group is 1.09 Å,[28] methyl–methyl carbon–hydrogen interactions, between tail groups, from opposite chains in the bilayer, are clearly possible (Scheme 1).

In this scheme hydrogens, from closely packed tail groups, could become partially positively polarized by nearby methyl carbons from opposite layers in a bilayer. The degree of polarization is a function of the vertical distance between tail group carbons. It should be noted that the D_{bt} value is less than 60% of the equilibrium C–C distance. Therefore, to achieve energy

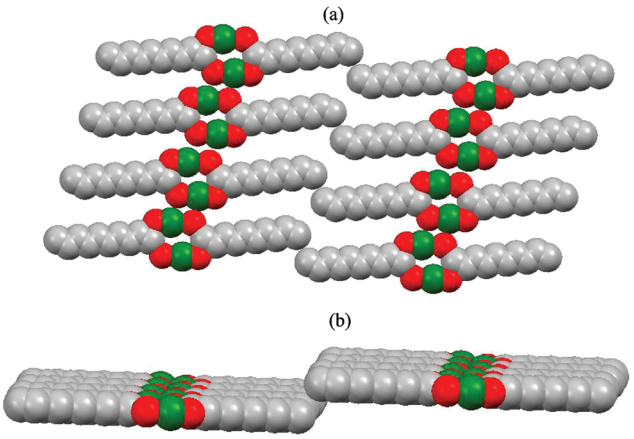

Fig. 6 (a) Aerial and (b) longitudinal view of lamellar structures for silver n-alkanoates.

Table 3 Melting points and density data for anhydrous silver n-alkanoates

n_c	Melting point/K (±0.01)	Lit.[ref. 5]/K	Density/g cm^{-3} (±0.05)
8	524.41	511.15	1.56
9	520.11	509.15	1.19
10	513.69	508.15	1.18
11	513.78	504.15	1.76
12	509.75	506.15	1.45
13	508.06	499.15	1.61
14	508.37	491.15	1.44
15	510.12	495.15	1.48
16	508.97	491.15	1.35
17	507.57	494.15	1.42
18	507.92	478.15	1.27
19	504.83	493.15	1.29
20	505.45	493.15	1.10

minimization and lattice stability, through low repulsive energy, hydrocarbon chains from adjacent layers, within a bilayer, must exist in different planes (Fig. 6). Hence, tail group carbon–hydrogen bonds will lengthen and weaken, as a result of repulsion between partially negative methyl carbons. This explains lower asymmetric methyl stretching frequencies and greater electron densities on methyl carbons for odd chain adducts.

The density of the compounds are in the range of 1.80–1.10 ± 0.05 g cm^{-3}, with odd chains having a higher value at all chain lengths studied (Table 3). The number of molecules per unit cell, Z is determined using the empirical formula: $Ag_2(CH_3(CH_2)_n\text{-}COO)_2$[6,7] in conjunction with measured densities and cell volumes. For $AgC_{8–16}$, Z = 1; for longer chains, the X-ray powder method is less sensitive, and hence Z values are multiples of this. Furthermore, odd–even alternation is observed in densities. Higher values for odd chains point to these adducts being more efficiently packed than their even chain length counterparts. However, as chain length increases the values converge. Clearly, there is competition between head group and van der Waal's interactions, between hydrocarbon chains. For short chain lengths, head group interactions predominate leading to higher densities and melting points, especially for more efficiently packed odd chains (Table 3). At high chain lengths a balance between these competing forces is achieved at n_C = ~23 when, the mass of the chain becomes comparable to the mass of the head group. At or near these chain lengths, even chains should then be more efficiently packed.

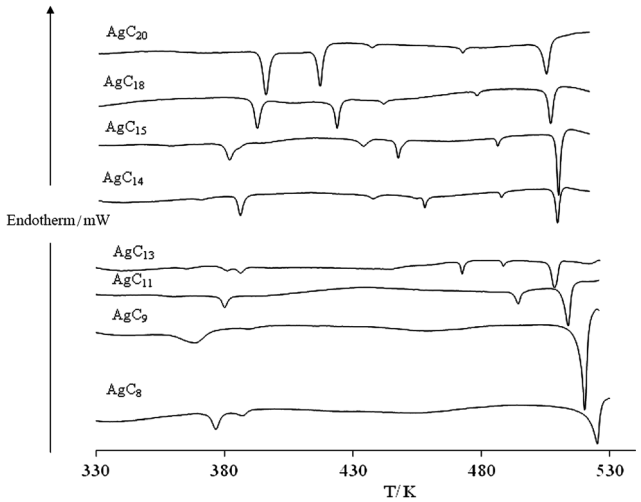

Fig. 7 Representtive D.S.C curves for selected anhydrous silver n-alkanoates.

Odd–even alternation then arises from the relative, vertical distances between planes. Clearly, the vertical distances between polymeric sheets are smaller for odd chains. Thus, a re-examination of Binnemans and coworkers powder X-ray data[5] for silver behenate, where intense, regularly spaced diffractions were observed at 2θ in the range of 25–35°, indicate that these reflections are likely to arise from interplanar interactions. The very regularity of these reflections supports this notion. These differences should be reflected in the thermal behaviour of these compounds.

Thus, representative D.S.C. heating curves, from 330–530 K, are shown in Fig. 7. There is a clear difference in the number of endothermic phase transitions observed for short (n_C = 8–10; three transitions) and long chains (n_C >11; > 3 transitions). The number of transitions and transition temperatures are in good agreement with those reported by Binnemans.[5] Clearly, the highest temperature transitions indicate fusion. As expected, the melting points of short chains are higher than for long chains because of the predominance of head group over van der Waal's interactions at these chain lengths. However, assignment of the other transitions presents a real, but not insurmountable, challenge. Because the compounds discolour and degrade on heating, polarized microscopic studies are unsuccessful. For $n_C \leq 11$, when head group interactions predominate, heating these adducts does not satisfy the condition for mesophase formation; that is, only when the two contending forces are roughly in balance will these compounds undergo mesomorphic transitions. Hence, the low temperature pre-melting transitions between 303–440 K are crystal-to-crystal transitions. For $n_C > 11$, van der Waal's forces become increasingly stronger with increasing chain length. However, on heating, these interactions decrease. Eventually, a rough balance between the two interactions is attained. Only then is mesomorphic transitions possible as observed between 440–480 K. As expected, the mesophase is formed at lower temperatures for higher chain lengths. At these transition temperatures, the head group is still intact and lends some order to the partial melt. As a consequence, the penultimate transition is not a mesophase-to-mesophase transition, as reported[5] but

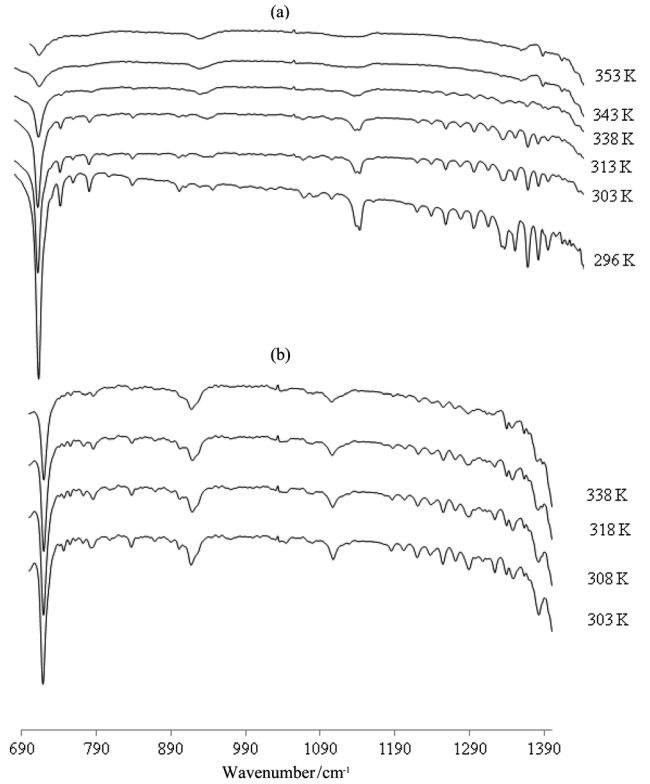

Fig. 8 Variable temperature infrared spectra for CH_2 progression bands.

rather a pre-melting transition which represents rearrangement of the head group and disruption of head group interactions. These types of transitions have been reported for other metal carboxylates.[29,30] Such a conclusion is supported by variable temperature infrared (Fig. 8). On heating between 296–353 K, (Fig. 8(a)) the intensity of methylene progression bands, in the region of 1390–790 cm^{-1}, is gradually reduced with increasing temperature. At 353 K the peaks completely disappear indicating partially molten hydrocarbon chains and loss of all-*trans* conformation. During the process, methylene groups are free to rotate about C–C bonds to give increased *gauche* conforms. These conformal changes give rise to crystal-to-crystal transitions, on the low temperature side of the D.S.C. trace. Also, the intensity of the peak at *ca.* 720 cm^{-1} is markedly reduced, with increasing temperature, indicating considerable disruption in chain packing. In the region of 1600–1360 cm^{-1}, where head group absorptions occur, there is a marked decease in intensities of ν_sCOO, ν_{as}COO and CH_2 rocking absorptions and appearance of a new peak at *ca.* 1565 cm^{-1}(Fig. 9(a). That is, at 353 K, the dimmer units begin to disassociate to give a more monodentate type structure (Scheme 2):

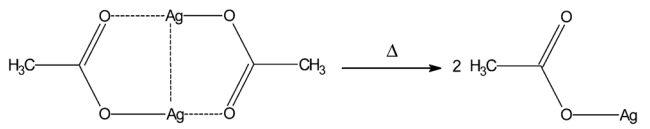

Scheme 2

Furthermore, methyl and methylene group absorptions decrease in intensity and are shifted to higher frequencies, with

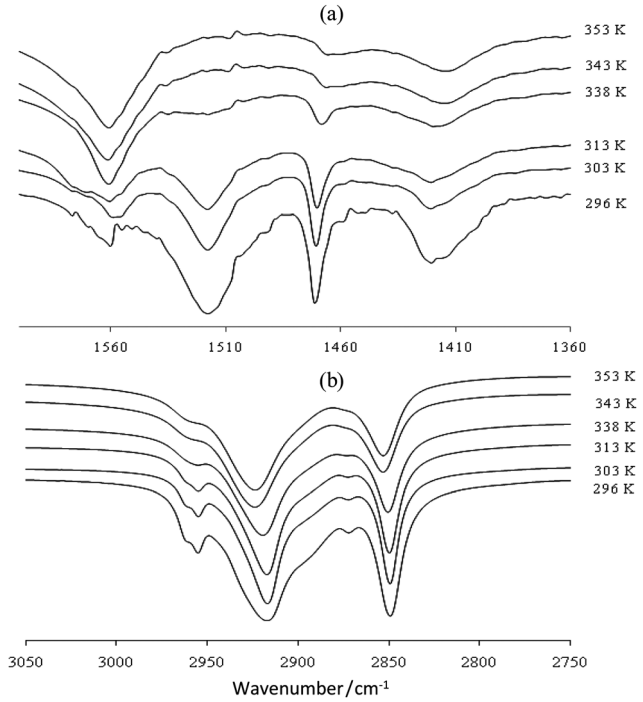

Fig. 9 Variable temperature infrared spectra for (a) COO and (b) CH_3 for selected silver n-alkanoate.

increasing temperature. The CH_3 asymmetric band, which is a doublet at room temperature because of van der Waal's interactions between hydrocarbon chains, collapses into a single low intensity band (Fig. 9(b)) which indicates increased rotational freedom of methyl groups resulting in the collapse of the polymeric sheets. On cooling (Fig. 8(b)), the methylene progression bands reappear though the spectrum is much changed from the room temperature one. That is, the process is not reversible. Beyond the melting point, the compounds rapidly decompose to metallic silver.

Conclusion

A homologous series of silver (I) n-alkanoates, for n_C = 8–20, inclusive, have been investigated by X-ray powder diffraction, Solid state ^{13}C NMR and Fourier transform infra-red spectroscopies. At ambient temperature, hydrocarbon chains are in the fully extended all-*trans* conformation and tilted *ca.* 75° to the metal basal plane. The chains are arranged as tail-to-tail bilayers, within a lamellar, and in such close proximity to allow methyl–methyl interactions, from different layers in the bilayer. Two carboxylate groups bind in a *syn–syn* type bridging bidentate mode to form an eight-membered structure, arranged in two dimensional polymeric sheets. Though the compounds are nearly isostructural, odd–even alternation in density, tail and, unusually, head group vibrational frequencies and electron densities are observed. These are ascribed to packing differences in the crystal lattice, between odd and even chains and the relative vertical distance between polymeric sheets, which are in different planes. Thus, odd chain length compounds, being of higher densities and increased molecular interactions are more efficiently packed.

Mesomorphic and crystal–crystal phase transitions are chain length depend and irreversible.

Experimental

The white microcrystalline solids were prepared by metathesis between sodium salt of n-alkanoic acids (Aldrich, 95+%), in ethanol, and an excess of aqueous silver nitrate (Aldrich, 99.9%) at *ca.* 343 K. The sodium salts were prepared by dissolving n-alkanoic acid in *ca.* 50 cm^3 of ethanol and combining this solution with *ca.*50 cm^3 of ethanol containing a stochiometric amount of sodium hydroxide (Aldrich, 99.9%). Subsequently, an aqueous solution of silver nitrate was added, drop-wise with stirring, to sodium alkanoate solution. This resulted in immediate precipitation of a white solid. After stirring for a further 30 min., at ambient temperature, the precipitate was collected by filtration, washed thrice with a solution of 1 : 1 acetone–methylene chloride mixture and vacuum dried for 24 h. The compounds were then stored in the dark (because of their sensitivity to light), in a desiccator over silica gel. (yield: *ca.* 90%).

FTIR-spectroscopy

Infrared spectra were recorded from ground samples, that were deposited on a quartz window, on a Bruker Tensor 37 FT-IR spectrometer in the range of 4000–400 cm^{-1} at a resolution of 1 cm^{-1}. Variable temperature measurements were made using a specially constructed devise which was calibrated for temperature control prior to each measurement.

Solid-state ^{13}C NMR spectroscopy

High resolution solid state spectra were collected, at room temperature, using a Bruker Avance 200 MHz spectrometer. Measurements were carried out at 50.32 MHz using CP and MAS with high-power ^1H decoupling for 3.6 μs pulse intervals and a 5.0 s recycle time using a 7 mm probe. Typically, 1024 scans were collected with a sweep width of 21.93 k Hz in 0.05 s. For acquisition, processing and plotting of the spectra, XWin NMR 3.5 computer software was used. TMS was used as reference at 0 ppm.

X-ray diffraction

Powder date were collected on a Bruker D5005 Diffractometer with nickel filtered Cu-Kα, radiation (λ = 1.54056 Å) from unground samples, finely deposited on standard plastic holders, specially designed to minimize preferred orientation. The X-ray tube was operated at 45 kV and 35 mA at a time per step of 2 s for 2 h between 2θ of 2–60°.

Differential scanning calorimetry (D.S.C.)

D.S.C. measurements were performed, in triplicate, on unground samples encased in standard alumina crucibles (100 μL), using a Setaram 560 system flushed with argon. The instrument was calibrated for temperature using pure indium, zinc and lead samples. Thermograms were collected from freshly prepared samples, each weighing between 2–4 ± 0.02 mg at a heating rate of 2.0 K $min.^{-1}$ between 323–523 K. Measurements were performed in triplicate.

Polarising light microscopy

Phase textures were examined under polarized light, on samples sandwiched between glass slides and coverslips, using a James Swift polarizing light microscope. The slides and coverslips were first immersed in an aqueous solution of 0.2% PVA. It was then heated to *ca.* 373 K, for a few minutes and cooled to ambient temperature, in order to produce good textures for examination.

Density measurements

Densities were determined at ambient temperature, in triplicate, by the mass–volume ratio method,[11] in n-hexane. The method gave excellent results, when used to determine known values for solid lead and lithium n-alkanoates.[12,13]

References

1 F. J. Buono and M. L. Feldman, *Kirk-Othmer Encyclopedia of Chemical Technology*, ed. H. F. Mark, D. F. Othmer, C. G. Overberger and G. T. Seaborg, Wiley, New York, 3rd edn, 1979, vol. 8, p. 34.
2 R. G. Bossert, *J. Chem. Educ.*, 1950, **27**, 10.
3 T. C. Huang, H. Toraya, T. N. Blanton and Y. Wu, *J. Appl. Crystallogr.*, 1993, **26**, 180.
4 V. Vand, A. Aitken and R. K. Campbell, *Acta Crystallogr.*, 1949, **2** (6), 398.
5 K. Binnemans, R. Van Deun, B. Thijs, I. Vanwelkenhuysen and I. Geuens, *Chem. Mater.*, 2004, **16**, 2021.
6 L. P. Olson, D. R. Whitcomb, M. Rajeswaran, T. N. Blanton and B. J. Stwertka, *Chem. Mater.*, 2006, **18**, 1667.
7 I. Weissbuch, J. Maewski, K. Kjaer, J. Als-Nielsen, M. Lahav and L. Leiserowitz, *J. Phys. Chem.*, 1993, **97**, 12848.
8 P. Pyyko, *Chem. Rev.*, 1997, **97**, 597.
9 F. A. Cotton, X. Feng, M. Matusg and R. Poli, *J. Am. Chem. Soc.*, 1988, **110**, 7077.
10 P. Pyykko and F. Mendizabal, *Chem.–Eur. J.*, 1997, **3**, 1458.
11 *Hand Book of Chemistry and Physics*, ed. R. C. Weast and D. E. Lide, CRC press, Florida, 49th edn, 1968–9, pp. F-73.
12 H. A. Ellis, N. A. S. White, I. Hassan and R. Ahamad, *J. Mol. Struct.*, 2002, **642**, 71.
13 H. A. Ellis, N. A. S. White, R. A. Taylor and P. T. Maragh, *J. Mol. Struct.*, 2005, **738**, 205.
14 R. A. Taylor, H. A. Ellis, P. T. Maragh and N. A. S. White, *J. Mol. Struct.*, 2006, **787**, 113.
15 H. Li, W. Bu, W. Qi and L. Wu, *J. Phys. Chem. B*, 2005, **109**, 21669.
16 N. A. S. White and H. A. Ellis, *J. Mol. Struct.*, 2008, **888**, 386.
17 S. J. Lee, S. W. Hon, H. J. Choi and K. Kim, *J. Phys. Chem. B*, 2002, **106**, 2892.
18 P. N. Nelson, H. A. Ellis and R. A. Taylor, *J. Mol. Struct.*, 2011, **986**, 10.
19 R. A. Taylor, H. A. Ellis and P. T. Maragh, *J. Mol. Struct.*, 2009, **921**, 118.
20 G. F. Marques, H. D. Burrows and M. G. Miguel, *J. Chem. Soc., Faraday Trans.*, 1998, **94** (12), 1729.
21 E. L Smith and M. D. Porter, *J. Phys. Chem.*, 1993, **97**, 8032.
22 T. Ishioka, Y. Shibata, M. Takahashi and I. Kanesaka, *Spectrochim. Acta, Part A*, 1998, **54**, 1811.
23 H. A. Ellis, *Mol. Cryst. Liq. Cryst.*, 1986, **139**, 281.
24 R. G. Snyder, *J. Mol. Spectrosc.*, 1961, **7**, 116.
25 H. A. Ellis and A. de Vries, *Mol. Cryst. Liq. Cryst.*, 1988, **163**, 133.
26 R. W. Corkery, *Phys. Chem. Chem. Phys.*, 2004, **6**, 1534.
27 B. P. Tolochko, S. V. Chernov, S. G. Nikitenko and D. R. Whitcomb, *Nucl. Instrum. Methods Phys. Res., Sect. A*, 1998, **405**, 428.
28 *Revised Nuffield Book of Data*, ed. H. Ellis, H. D. Harrison and H. D B. Jenkins, Longman, Aylesbury, 4th edn, 1984, ch. 4.7, pp. 52.
29 M. R. Barr, B. A. Dunnel and R. F. Grant, *Can. J. Chem.*, 1963, **41**, 1188.
30 G. Berchiesi, M. A. Berchiesi, G. G. Lobbia and D. Leonesi, *Gazz. Chim. Ital.*, 1976, **106**, 549.

